$$[S] = \begin{vmatrix} 0 & 0 & S'_{13} - S'_{14}\sin 2\theta & S'_{14}\cos 2\theta \\ 0 & 0 & S'_{14}\cos 2\theta & S'_{13} + S'_{14}\sin 2\theta \\ S'_{13} + S'_{14}\sin 2\theta & -S'_{14}\cos 2\theta & 0 & 0 \\ -S'_{14}\cos 2\theta & S'_{13} - S'_{14}\sin 2\theta & 0 & 0 \end{vmatrix}$$

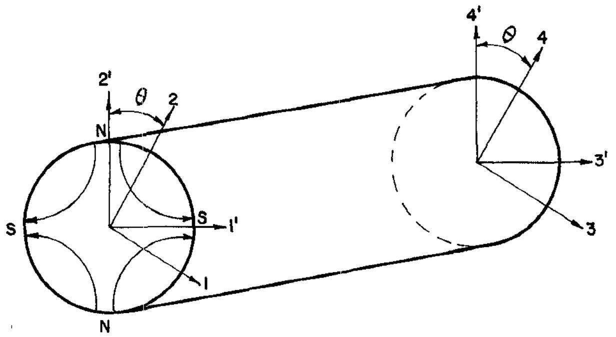

Fig. 2. Schematic diagram of circular waveguide with a quadrupole dc magnetic field.

and lower signs in the matrix (2) correspond to two directions of dc magnetic field or two directions of propagation. When $k = \sqrt{2}/2$, we have the case of a quarter wave plate.

Let us apply now to a circular gyromagnetic waveguide (Fig. 2). Write down the matrix $[S']$ for the ideally matched waveguide with the ports $1', 2', 3'$, and $4'$, lying in the antiplanes of symmetry

$$[S'] = \begin{vmatrix} 0 & 0 & S'_{13} & S'_{14} \\ 0 & 0 & S'_{14} & S'_{13} \\ S'_{13} & -S'_{14} & 0 & 0 \\ -S'_{14} & S'_{13} & 0 & 0 \end{vmatrix}.$$

To find the matrix $[S]$ for the waveguide with the ports 1, 2, 3, and 4, rotated at an angle θ about the ports $1', 2', 3'$, and $4'$, consider, for example, a wave a_1 in the port 1. It may be presented as a vector sum of the two components a'_1 and a'_2 in the ports $1'$ and $2'$

$$a'_1 = a_1 \cos\theta, \quad a'_2 = -a_1 \sin\theta.$$

Using the matrix relation between reflected and incident waves

$$[b'] = [S'][a']$$

we have

$$\begin{aligned} b'_3 &= a_1 S'_{13}\cos\theta + a_1 S'_{14}\sin\theta \\ b'_4 &= -a_1 S'_{13}\sin\theta - a_1 S'_{14}\cos\theta \end{aligned}.$$

The sum of the projections of b'_3 and b'_4 on the port 3 is

$$b_3 = b'_3\cos\theta - b'_4\sin\theta.$$

Now we may derive the element S_{31}

$$S_{31} = b_3/a_1 = S'_{13} + S'_{14}\sin 2\theta.$$

The other elements of $[S]$ are calculated analogously. Thus, the desired scattering matrix has the form as in the matrix shown at the top of the page.

The elements S_{13}, S_{31}, S_{24}, and S_{42} consist of two parts: reciprocal S'_{13} and nonreciprocal $S'_{14}\sin 2\theta$. The latter depends on the angle θ.

When $S'_{13} = 0$, we obtain the matrix for the quadrupole half-wave plate

$$[S] = S'_{14}\begin{vmatrix} 0 & 0 & -\sin 2\theta & \cos 2\theta \\ 0 & 0 & \cos 2\theta & \sin 2\theta \\ \sin 2\theta & -\cos 2\theta & 0 & 0 \\ -\cos 2\theta & -\sin 2\theta & 0 & 0 \end{vmatrix}. \quad (3)$$

If $|S'_{14}| = 1$, it is the case of a nondissipative waveguide. With $\theta = \theta' + \pi/4$ and $S'_{14} = 1$ the matrix (3) is transformed into the matrix, deduced in [2] by another method.

The method is applicable to symmetrical devices with gyroelectric media as well.

REFERENCES

[1] V. A. Dmitriyev, "Color group approach to matrix description of symmetrical waveguide junctions and coupled lines with gyrotropic media," *IEEE Trans. Microwave Theory Tech.*, vol. 43, no. 12, Dec. 1995.

[2] J. Helszajn, W. A. Leeson, D. J. Lynch, B. C. O'Donnell, "Normal mode nomenclature of quadrupole gyromagnetic waveguides," *IEEE Trans. Microwave Theory Tech.*, vol. 39, pp. 461–470, Mar. 1991.

[3] R. McWeeny, *Symmetry. An Introduction to Group Theory and its Applications.* Oxford: Pergamon, 1963.

A New Approach for Analysis of Resonant Structures Based on the Spatial Finite-Difference and Temporal Differential Formulation

Zhizhang Chen and Alan Ming Keung Chan

***Abstract*—This paper presents a new procedure for analyzing resonant structures using the spatial finite-difference and temporal differential formulation. Unlike the conventional finite-difference time-domain methods, the finite-difference are only enforced in the spatial domain for Maxwell's equations. The time-domain differentials of Maxwell's equations are kept, resulting in a system of first-order differential equations. In consequence, a resonant structure problem can be formulated in the eigenvalue problem form and resonant modes are obtained by solving the corresponding eigenvalue problem directly. It is shown that the coefficients of the matrix for the eigenvalue problem can be simply obtained from the finite-difference time-domain formulation. As a result, an efficient alternative way of using the finite-difference time-domain approach to solve the resonant structure problems is presented. The algorithm is applied to metallic waveguide structures and the numerical results agree well with those from other techniques.**

Manuscript received August 25, 1995; December 18, 1995. This work was supported by the Natural Science and Engineering Research Council (NSERC) of Canada.

The authors are with the Department of Electrical Engineering, Technical University of Nova Scotia, Halifax, Nova Scotia, B3J 2X4 Canada.

Publisher Item Identifier S 0018-9480(96)02331-9.

I. Introduction

Recent development of the recursive time-domain formulations, such as the finite-difference time-domain (FDTD) method, have presented the very powerful numerical tools in solving electromagnetic structures in time domain. They can account for very complicated structures to which the analytical solutions are not applicable. The theory and applications of the FDTD method and a list of extensive reference can be found in [1].

Normally, when the conventional FDTD scheme is employed to resonant structure problems, an excitation at a predetermined location is imposed and the response (output) at another chosen location is recorded for the entire simulation. Discrete Fourier transform (DFT) is then performed on the output data to obtain the frequency response (spectrum) and a resonant frequency is identified by observing a peak over the frequency spectrum. If the mode distribution is required, DFT over the whole spatial domain at the resonant frequency identified has to be performed, or alternatively, another simulation with the sinusoidal excitation of the resonant frequency needs to be carried out.

The simulation processes as such have experienced the following problems: 1) if either excitation points or output points are located at or nearby null field points of a mode, the mode can not be well extracted; 2) for a high-Q structure, a long iteration is required to obtain the sufficient accuracy, resulting in the large CPU time, and 3) the CPU time and memory is independent of the number of modes required. In this paper, we present a new procedure which circumvent the above problems while still enable us to determine resonant modes and their frequencies based on the time domain formulation.

II. Spatial Finite-Difference and Temporal Differential (SFDTD) Form of Maxwell's Equations

For the sake of simplicity, a stationary, lossless and sourceless medium is assumed with the notation that the principle can be easily extended to other cases. The Maxwell's equations can then be expressed as

$$\frac{\partial \boldsymbol{E}}{\partial t} = -\frac{1}{\epsilon}\nabla \times \boldsymbol{H} \tag{1}$$

$$\frac{\partial \boldsymbol{H}}{\partial t} = \frac{1}{\mu}\nabla \times \boldsymbol{E}. \tag{2}$$

Now, if we use the Yee's grid arrangement for approximating the curl operation "$\nabla\times$" with the central finite-differences in the spatial domain [2] while maintaining the time-domain differentials in Maxwell's equations, the above equations can be written as

$$\frac{d\boldsymbol{E}}{dt} = \boldsymbol{D}_1\boldsymbol{H} \tag{3}$$

$$\frac{d\boldsymbol{H}}{dt} = \boldsymbol{D}_2\boldsymbol{E} \tag{4}$$

where $\boldsymbol{E} = [\cdots, E_x(t, i_x+\frac{1}{2}, i_y, i_z), \cdots, E_y(t, i_x, i_y+\frac{1}{2}, i_z), \cdots, E_z(t, i_x, i_y, i_z+\frac{1}{2}), \cdots]^T$ and $\boldsymbol{H} = [\cdots, H_x(t, i_x, i_y+\frac{1}{2}, i_z+\frac{1}{2}), \cdots, H_y(t, i_x+\frac{1}{2}, i_y, i_z+\frac{1}{2}), \cdots, H_z(t, i_x+\frac{1}{2}, i_y+\frac{1}{2}, i_z), \cdots]^T$. In other words, $\boldsymbol{E}$ and $\boldsymbol{H}$ are now the one-column vectors whose components are the electric and magnetic field components defined on the grid points at any arbitrary time t. $\boldsymbol{D}_1$ is the $N_e \times N_h$ coefficient matrix and $\boldsymbol{D}_2$ is the $N_h \times N_e$ coefficient matrix, resulting from the finite-difference approximation processes in the spatial domain. N_e is the total number of E nodes while N_h is the total number of H modes. Note that $\boldsymbol{D}_1$ and $\boldsymbol{D}_2$ are both sparse matrices due to the localized finite-difference scheme.

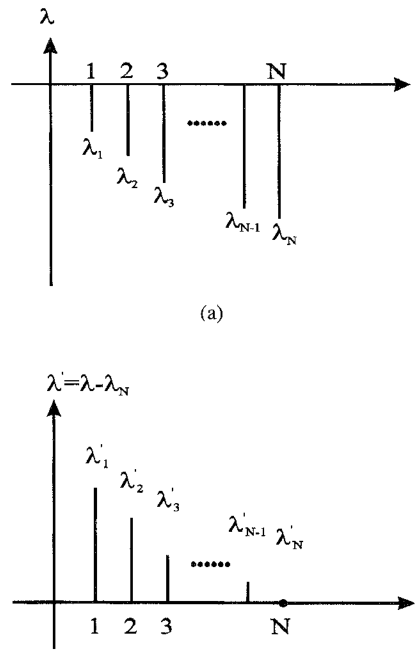

(a)

(b)

Fig. 1. Eigenvalue distributions of (a) the original problem and (b) the transformed problem.

Since the above formulations are the result of spatially finite-differencing Maxwell's equations without modifying the temporal differentials, we term them the "spatial finite-difference and temporal differential (SFDTD) formulation" of Maxwell's equations.

By comparing the SFDTD formulations with the FDTD formulations [3], one can see that the SFDTD formulation can be considered as the limiting case of the FDTD scheme with the time step $\delta t \to 0$. Consequently, the element values of $\boldsymbol{D}_1$ and $\boldsymbol{D}_2$ can be obtained directly from the FDTD formulations by simply excluding the coefficients which are resulted from the time-domain finite-differences. In other words, we now present an alternative way of using the FDTD scheme to obtain the field solutions by solving the SFDTD equations instead of the direct simulation. As will be seen in the next section, it avoids the problems with direct simulation mentioned in the introduction.

Equations (3) and (4) very much resemble the transmission line equations with only the difference that they are expressed in a matrix form. They can be solved in a way similar to the one-dimensional transmission line equations.

III. Solutions of Maxwell's Equations in the SFDTD Form

By combining equations (3) and (4), we obtain

$$\frac{d^2\boldsymbol{E}}{dt^2} = \boldsymbol{D}_1\boldsymbol{D}_2\boldsymbol{E} = \boldsymbol{D}_{12}\boldsymbol{E} \tag{5}$$

where $\boldsymbol{D}_{12} = \boldsymbol{D}_1 \cdot \boldsymbol{D}_2$ is an $N_e \times N_e$ sparse matrix. The above equation is essentially the time-domain wave equation in the SFDTD form. It is, however, derived directly from Maxwell's equations and thus it takes into account of the coupling among all the components of $\boldsymbol{E}$ and $\boldsymbol{H}$.

Suppose $\boldsymbol{D}$ is the $N_e \times N_e$ diagonal matrix with its jth diagonal element λ_j ($j = 1, 2, \cdots, N_e$) being the jth eigenvalue of $\boldsymbol{D}_{12}$. $\boldsymbol{Y}$ is the $N_e \times N_e$ modal matrix of $\boldsymbol{D}_{12}$, i.e., the matrix whose column are the eigenvectors $\boldsymbol{y}_j$ of $\boldsymbol{D}_{12}$. The solution of the above equation

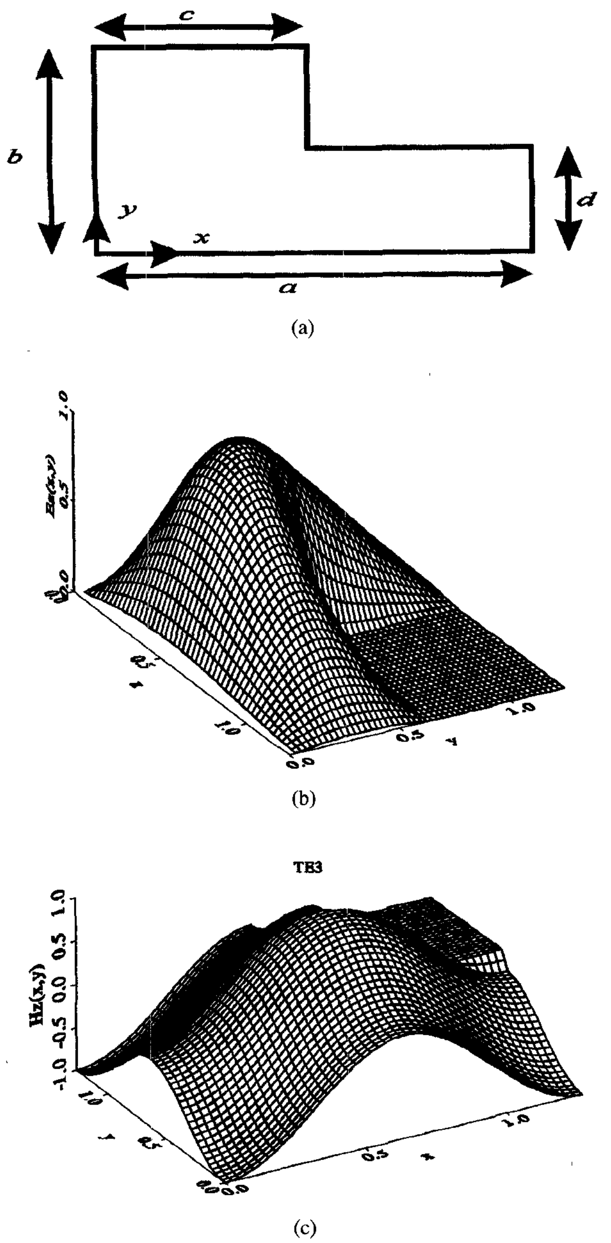

Fig. 2. (a) Cross section of the L-shaped waveguide. (b) TM1 mode distribution. (c) TE3 mode distribution.

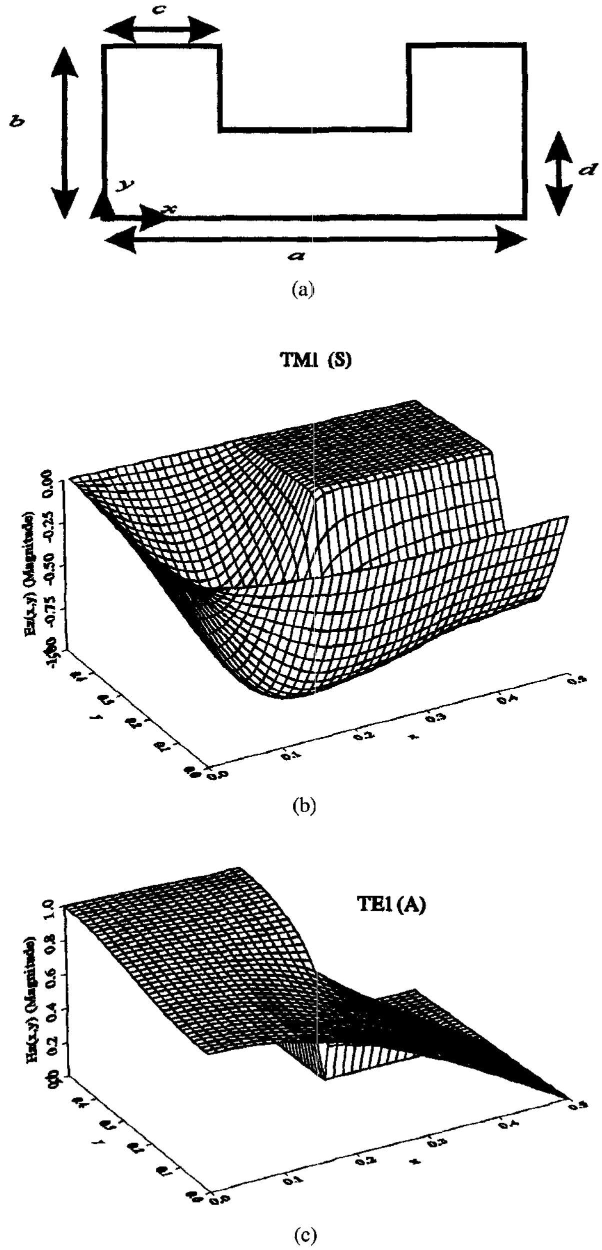

Fig. 3. (a) Cross section of the single-ridged waveguide. (b) TM1 (S) mode distribution. (c) TE3 (A) mode distribution for half the waveguide.

is then [3]

$$\begin{aligned}\boldsymbol{E} &= \boldsymbol{Y}\mathrm{e}^{\boldsymbol{D}^{\frac{1}{2}}t}\boldsymbol{a} \\ &= a_1\mathrm{e}^{\sqrt{\lambda_1}t}\boldsymbol{y}_1 + a_2\mathrm{e}^{\sqrt{\lambda_2}t}\boldsymbol{y}_2 + \cdots + a_{N_e}\mathrm{e}^{\sqrt{\lambda_{N_e}}t}\boldsymbol{y}_{N_e} \qquad (6)\end{aligned}$$

where one column constant vector $\boldsymbol{a} = [a_1, a_2, \cdots, a_{N_e}]^T$ is determined by the initial condition of $\boldsymbol{E}$. (Note that here we assume $\boldsymbol{D}_{12}$ is nondefective. If it is defective, generalized eigenvectors can be used, albeit the above equation will be a bit more complicated.)

The above equation shows that the numerical waves in the discretized space consist of: N_e eigenmodes whose amplitudes are modulated by $\mathrm{e}^{\sqrt{\lambda_j}t}$ with frequency of $\mathrm{Im}(\sqrt{\lambda_j})$. The spatial eigendistributions are represented by $\boldsymbol{y}_j$. They are dependent on the configuration of the discrete system, but independent of excitations. The initial conditions simply decide the size of each modal components by exciting each individual eigenmode with some amplitude a_j.

It is worth to mention here that a similar solution form exists for $\boldsymbol{H}$. The choice for selecting $\boldsymbol{E}$ or $\boldsymbol{H}$ for solutions is rather dependent on the personal preference. In our case, we made the choice based on the comparison between N_e and N_h. If $N_e < N_h$, choose $\boldsymbol{E}$. If $N_h > N_e$, choose $\boldsymbol{H}$. In this way, the smaller size of $\boldsymbol{D}_{12}$ can be obtained, resulting in smaller computation expenditure. Nevertheless, $\boldsymbol{H}$ can be obtained from the known $\boldsymbol{E}$ and vice versa through (3) or (4).

IV. Applications to Resonant Structures

When STDFD is applied to a resonant structure, naturally, $\mathrm{Im}(\sqrt{\lambda_j})$ will be the resonant frequency and eigenvector $\boldsymbol{y}_j$ is the corresponding mode distribution. As a result, to solve for a resonant structure with SFDTD is in fact to solve an eigenvalue problem in respect to the matrix $\boldsymbol{D}_{12}$.

TABLE I
EIGEN-RELATIONSHIP BETWEEN THE ORIGINAL MATRIX AND THE TRANSFORMED MATRIX

	Matrix	Eigenvalue	relationship	Eigenvector
Original	$\mathbf{D}_{12}$	l_p	$l_p = l'_p - l_N$	y_p
Transformed	$\mathbf{D}'_{12}$	l'_p		y_p

TABLE II
COMPARISON OF THE CUTOFF WAVENUMBER k_c (rad/cm) FOR THE L-SHAPED WAVEGUIDE ($a = b = 1.27$ cm, $c = d = a/2$)

						Difference between the present &			
Mode	SIE[8]	FD-CGM[9]	FD-SIC[10]	Present	Analytic	SIE	FD-CGM	FD-SIC	Analytic
TM_1	4.8677	4.80	4.8949	4.8832	------	0.32%	1.73%	0.24%	-------
TM_2	6.1361	6.07	6.1350	6.1383	------	0.04%	1.13%	0.05%	-------
TM_3	6.9908	6.92	6.9921	6.9908	6.9967	0.00%	1.02%	0.02%	0.08%
TM_4	8.5525	8.61	8.5458	8.5475	------	0.06%	0.73%	0.02%	-------
TM_5	-------	9.72	8.8940	8.8915	------	-------	8.52%	0.03%	-------
TE_1	1.8917	1.88	1.9111	1.9158	------	1.27%	1.90%	0.25%	-------
TE_2	2.9159	2.95	2.9600	2.9599	------	1.51%	0.34%	0.00%	-------
TE_3	4.8755	4.89	4.9452	4.9441	4.9474	1.41%	1.11%	0.02%	0.04%
TE_4	------	------	4.9452	4.9442	4.9474	-------	--------	0.02%	0.06%
TE_5	5.2463	5.26	5.3128	5.3116	-------	1.24%	0.98%	0.02%	--------

TABLE III
COMPARISON OF THE CUTOFF WAVENUMBER k_c (rad/cm) FOR THE SINGLE-RIDGED WAVEGUIDE ($a = 1.0$ cm, $b = 0.5$ cm, $c = d = 0.25$ cm)

						Differences between the present and		
Mode	Type	SIE[ ]	FD-CGM[ ]	FD-SIC[ ]	Present	SIE	FD-CGM	FD-SIC
TM_1	S	12.038	12.05	12.145	12.145	0.89%	0.79%	0.00%
TM_2	A	12.294	12.32	12.433	12.404	0.89%	0.68%	0.23%
TM_3	S	13.996	13.86	14.004	14.014	0.12%	1.11%	0.07%
TM_4	A	15.587	15.34	15.583	15.591	0.03%	1.64%	0.05%
TM_5	S	-------	16.28	16.640	16.695	-------	2.55%	0.32%
TE_1	A	2.2496	2.23	2.2422	2.2537	0.18%	1.06%	0.51%
TE_2	S	4.9436	4.78	4.8543	4.8662	1.57%	1.80%	0.24%
TE_3	A	6.5189	6.40	6.4476	6.4608	0.89%	0.95%	0.20%
TE_4	S	7.5642	7.48	7.5185	7.5182	0.61%	0.51%	0.00%
TE_5	A	-------	9.71	9.8314	9.8207	-------	1.14%	0.10%

To solve the eigenvalues of D_{12}, many methods can be applied. Since we are more concerned about the dominant modes (lower order modes) in most cases and D_{12} is a sparse matrix, many of the sparsity-based power methods can be used. In this paper, the simultaneous iteration (SI) technique described in [4] is used in order to have high efficiency and computation speed. However, the technique is only applicable to the problem where the eigenvalues of largest-magnitude are to be found. In our case, the dominant modes correspond to the eigenvalues of least-magnitudes as they have the lowest resonant frequencies. Therefore, a transform is needed to convert the eigenvalues of least-magnitude in the original problem to the eigenvalues of largest-magnitude in another modified problem. Inversed power method or its variations [3] may be used. However, they involve the computation for the inversion of a large matrix (or equivalents) which may consume a lot of CPU time. In the following paragraph, we will describe a simple transform technique to reach the solutions.

Suppose that the distribution of the eigenvalues can be graphically represented as shown in Fig. 1(a). As we can see, the dominant modes have the least-magnitude eigenvalues since

$$\boldsymbol{D}_{12}\boldsymbol{y}_j = \lambda_j \boldsymbol{y}_j \tag{7}$$

then

$$\boldsymbol{D}'_{12}\boldsymbol{y}_j = \lambda'_j \boldsymbol{y}_j$$

where $\lambda' = \lambda - \lambda_N$ and $\boldsymbol{D}'_{12} = \boldsymbol{D}_{12} - \lambda_N \boldsymbol{I}$ ($\boldsymbol{I}$ is the unity matrix and $N = N_e$ or N_h). λ_N is the eigenvalue of the largest-magnitude of the original matrix $\boldsymbol{D}_{12}$ and can be obtained by applying the SI technique to $\boldsymbol{D}_{12}$.

The new eigenvalue (λ') distribution is shown in Fig. 1(b). It can be seen that the dominant modes correspond to the new eigenvalues which have the largest-magnitudes. The SI technique as mentioned before can then be applied to solve the eigenvalues for the dominant modes. Table I shows that eigenvalue relationships between the new matrix and original matrix. Note that the transform does not change the eigenvectors.

V. Numerical Results

The rectangular hollow metallic waveguide and many of its variations, such as the ridged waveguides, [5], [6], for wide bandwidth operations, are commonly used in microwave systems [7]. Most research on the related topics has been performed and different techniques have been used to obtain the cutoff frequencies and mode field distributions. The techniques include surface integral equation (SIE) method [8], the finite-difference method coupled with the conjugate gradient approach (FD-CGM) [9] and the finite-difference method with the simultaneous iteration and Chebyshev acceleration technique (FD-SIC) [10]. With the results obtained from these techniques as references, evaluations can be made on the accuracy of the present method. In the following examples, metallic waveguides with rectangular boundaries (which become resonant at the cutoff frequencies) are analyzed.

The first example is the L-shaped waveguide with $a = b = 1.27$ cm and $c = d = a/2$, depicted in Fig. 2(a). A 50 × 50 grid is used to calculate a few dominant cutoff wavenumbers of the TM and TE modes. The numerical results are shown in Table II and in Fig. 2. Note that the cutoff wavenumber k_c equals to ω_c/c with c being the speed of the light in the medium.

The second example is the single-ridge waveguide with $a = 1.0$ cm, $b = 0.5$ cm, and $c = d = 0.25$ cm, depicted in Fig. 3(a). Again, a 50 × 50 grid is used to calculate a few dominant cut-off wavenumbers of the TM and TE modes. The numerical results are shown in Table III and in Fig. 3 where "S" and "A" in the brackets stand for the "symmetric" and "asymmetric" modes, respectively.

From Tables II and III, it is seen that for most of the modes in both examples, the results from the different techniques agree well with the discrepancies of less than 2%. Whenever the analytical solutions are available, the errors of the present method are less than 1%. The field distributions obtained also agree very well with the results obtained with the other techniques [10].

VI. Conclusion

In this paper, a new alternative procedure of using the finite-difference time-domain method to analyze resonant structures has been proposed. It is based on the spatial finite-difference and temporal differential formulation of Maxwell's equations. The solutions are obtained in a manner very much similar to the frequency-domain methods by solving an eigenvalue problem. Therefore, the method becomes more efficient than the direct simulation with FDTD method. As a result, matrix computation techniques employed in the frequency-domain methods can be applied.

References

[1] A. Taflove, "Review of the formulation and applications of the finite-difference time-domain method for numerical modelling of electromagnetic wave interactions with arbitrary structures," *Wave Motion*, vol. 10, pp. 547–582, Dec. 1988.

[2] K. S. Yee, "Numerical solution of initial boundary value problems involving Maxwell's equations in isotropic media," *IEEE Trans. Antennas Propagat.*, vol. 14, pp. 302–307, May 1966.

[3] H. Anton, *Elementary Linear Algebra.* New York: Wiley, 1994.

[4] L. Wang and A. Semlyen, "Application of sparse eigenvalue techniques to the small signal stability analysis of large power systems," in *Proc. 1989 IEEE Power Industry Computer Applicat. Conf.*, Seattle, WA, May 1–5, 1989, pp. 635–642.

[5] J. P. Montgomery, "On the complete eigenvalue solution of ridged waveguide," *IEEE Trans. Microwave Theory Tech.*, vol. MTT-19, no. 6, pp. 547–555, June 1971.

[6] Y. Utsumi, "Variational analysis of ridged waveguide modes," *IEEE Trans. Microwave Theory Tech.*, vol. MTT-33, no. 2, pp. 111–120, Feb. 1985.

[7] X. P. Liang, K. A. Zaki, and A. E. Atia, "Dual mode coupling by square corner cut in resonators and filters," *IEEE Trans. Microwave Theory Tech.*, vol. 40, No. 12, pp. 2294–2302, Dec. 1992.

[8] M. Swaminathan, E. Arvas, T. K. Sarkar, and A. R. Djordjevic, "Computation of cutoff wavenumbers of TE and TM modes in waveguides of arbitrary cross-sections using a surface integral equation," *IEEE Trans. Microwave Theory Tech.*, vol. 38, no. 2, pp. 154–159, Feb. 1990.

[9] T. K. Sarkar, K. Anthar, E. Arvas, M. Manela, and R. Lade, "Computation of the propagation characteristics of TE and TM modes in arbitrarily shaped hollow waveguides utilizing the conjugate gradient method," *J. Electromagn. Wave Appl.*, vol. 3, no. 2, pp. 143–165, 1989.

[10] J.-M. Guan and C.-C. Su, "Analysis of metallic waveguides with rectangular boundaries by using the finite-difference method and the simultaneous iteration with the Chebyshev acceleration," *IEEE Trans. Microwave Theory Tech.*, vol. 43, no. 2, pp. 374–382, Feb. 1995.